

PARAMETRIC SYSTEM ANALYSIS IN CHARGE COUPLED DEVICE IMAGING APPLICATIONS

RALPH WIGHT
Director, Advanced Development

Imaging Systems Division
Federal Systems Group
Fairchild Camera & Instrument Corp.

ABSTRACT

The advent of Charge Coupled Device (CCD) imaging sensors has required the development of specific techniques of parametric analysis which are of use to systems designers and engineers in the synthesis of electro-optical imaging systems employing these sensors. This paper describes the development and application of several of these methods and techniques including: The evaluation of a photometric/radiometric model, together with a simple method for conversion from one domain to the other; a description of a signal-to-noise model of particular applicability to this type of sensor; an analysis of operational parameter space which includes modulation considerations, noise considerations detective quantum efficiency evaluation and signal characteristics; and illustrative examples of how the techniques described may be applied.

INTRODUCTION

The applicability of Charge Coupled Device imaging sensors to specific system requirements can be readily assessed, provided the parametric analysis of the system is conducted along proper lines. In order for this to be done, it is necessary to understand the interrelationships among the functional characteristics of the devices contemplated for use in a specific application. Pre-ordained system specifications tend to force solutions to follow in such a way that if the system designer is not cautious, several device operational characteristics which are mutually exclusive (although attainable individually) may become part of the analysis. The object of this paper is to provide the Electro-Optical System Designer with the analytic tools needed for the parametric design of imaging systems employing Charge Coupled Devices.

PHOTOMETRIC/RADIOMETRIC RELATIONSHIPS

When Charge Coupled Device imaging sensors (CCD's) are used as radiation detectors, it is essential to know how the responsivity of the sensor matches the radiation output of the scene being viewed. Under unusual circumstances, the system designer has control over both the sensor and the source of scene illumination, and can therefore optimize the combination. More usually, however, the sensor must perform when coupled with naturally illuminated objects. Since scene illuminance related to such natural conditions as "sunlight", "moonlight", "starlight", etc. is generally stated in photometric units (foot candles), while electro-optical system performance is most easily evaluated on the basis of radiometric units (watts per square centimeter), it has proved highly useful in parametric analysis to develop a simple scheme by which the former may be readily converted to the latter for any given blackbody color temperature.

The relationship of blackbody source temperature (T) in degrees Kelvin is related to luminosity (lumens/watt) as shown in Figure 1.

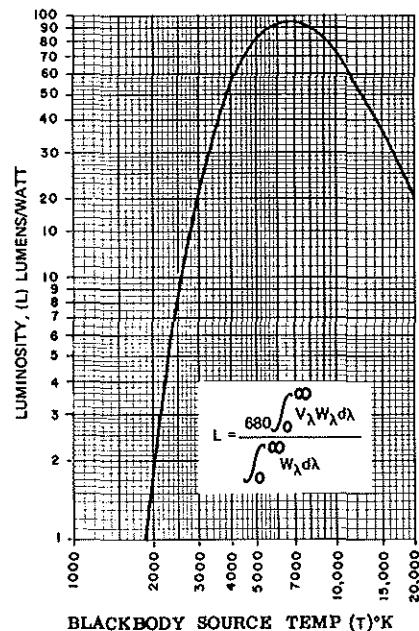


FIGURE 1. LUMINOSITY AS A FUNCTION OF BLACKBODY TEMPERATURE

Since a foot candle is defined as one lumen per square foot, a conversion to watts per square centimeter can be made using the relationship:

$$W \cdot \text{cm}^{-2} = \frac{1}{9} \text{FC}$$

Where I is the illuminance in foot candles, and P a photometric/radiometric conversion factor as shown in Figure 2 where:

$$P = \frac{0.001076}{\text{Luminosity in Lumens/watt}}$$

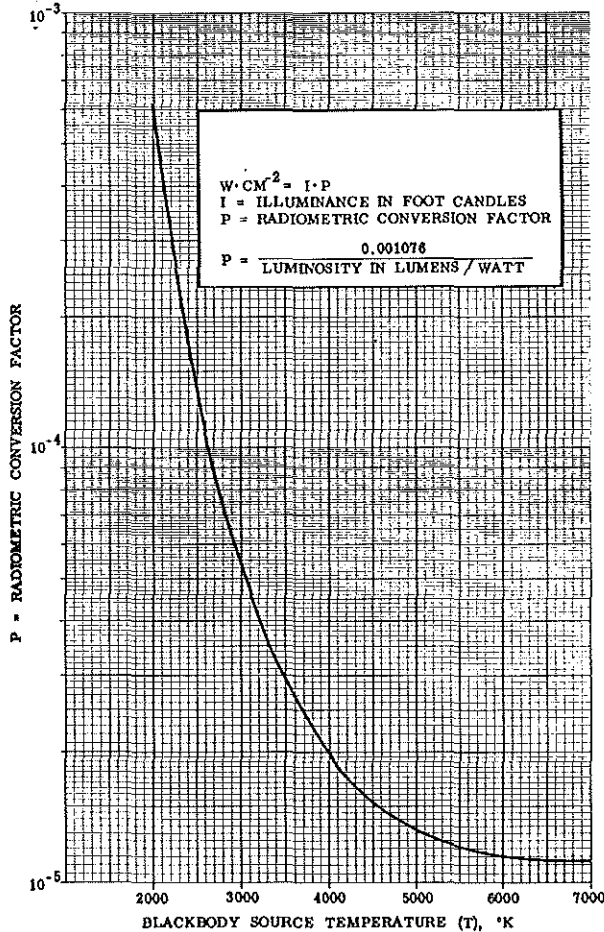


FIGURE 2. PHOTOMETRIC/RADIOMETRIC CONVERSION EXPRESSION

The desirability of going through this procedure, rather than simply working in radiometric units to begin with results from the fact that insofar as a spectrally unflat sensor working in conjunction with spectrally different sources is concerned, watts, like Orwell's animals, are not really all equal. It is necessary to evaluate sensor sensitivity to sources of different blackbody color temperatures. It is also necessary to take the blackbody color temperature of the illumination into account when performing system analysis. The cascade and integration of the appropriate values over the spectral region of interest yield radiometric values of parametric validity and utility, without the necessity for performing extended integrations of cascaded values for sensor response and illuminance data in the form of $W \text{ cm}^{-2} \cdot \text{Sr}^{-1} \cdot \mu\text{m}^{-1}$.

When dealing with "sunlight", the blackbody color temperature selected as representative will differ depending upon the atmospheric path. For example, instruments in a high flying aircraft may see the earth illuminated by a source effectively significantly cooler than 5000°K while under other circumstances, solar illumination more closely approaches 6000°K. (Ref 1). The blackbody color temperature of scene illumination also varies widely with solar altitude. This change results from a variety of causes, but conforms generally to the data presented in Figure 3. The 15°-0° plane is one tilted 15 degrees from perpendicular with the sun "behind" the observer. It is apparent from the figure that as the sun approaches the horizon, the blackbody color temperature of the illumination decreases so that, at sunset, one is likely dealing with illumination in the 2854°K (nominal tungsten) color temperature region.

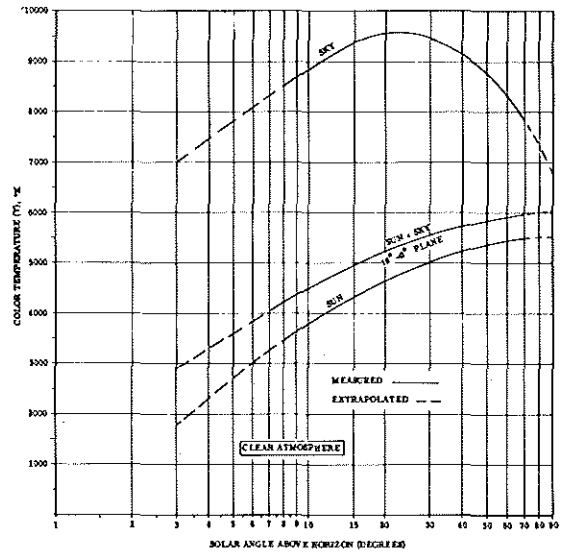


FIGURE 3. RELATIONSHIPS AMONG SOLAR ELEVATION ANGLE AND ILLUMINATION COLOR TEMPERATURE

Because of their high level of sensitivity CCD image sensors have been hypothesized for use in low light level applications. The moving image integrating mode device (described in another paper presented at this conference) is one example of a sensor especially designed for low light level use. Illumination conditions change not only quantitatively, but qualitatively when natural light levels fall. When the sun is well below the horizon, and the moon is taken as the chief source of illumination, the resultant blackbody color temperature may be seen to be highly dependent upon the altitude and phase of the moon (Ref 2). This is shown in Figure 4 where the relative radiance of different lunar illumination conditions are shown as a function of wavelength. Plotted together with the illumination data are straight-line approximations of blackbody curve segments for the indicated spectral interval. These approximations were obtained by joining the 500 nm and 1100 nm portions of the respective blackbody curves by a straight line. As is shown in the Figure, the blackbody color temperature varies from about 2854°K, with no moon, to about 5400°K with nearly full moon at a 45 degree altitude.

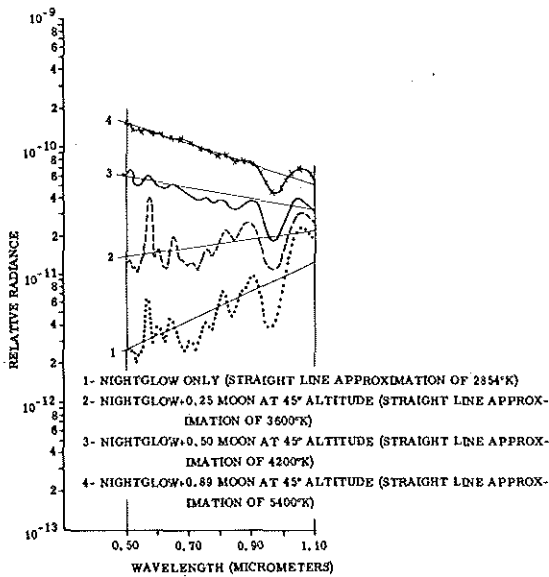


FIGURE 4. RELATIONSHIPS AMONG ILLUMINATION CONDITIONS AND BLACKBODY SOURCE TEMPERATURE

The extreme condition represented by the illumination received from starlight and airglow alone may be evaluated through the use of Figure 5. The Figure shows the relative number of photons emitted by a blackbody as a function of wave length. It also has plotted on it (at the same scale) the relative number of photons collected at the surface of the earth from the night sky (starlight plus airglow) (Ref 3). By mentally "sliding" the plot of night sky photons over the figure, one may arrive at a "best fit" between the data. It is apparent that this fit occurs somewhere in the region of 2854°K–3000°K.

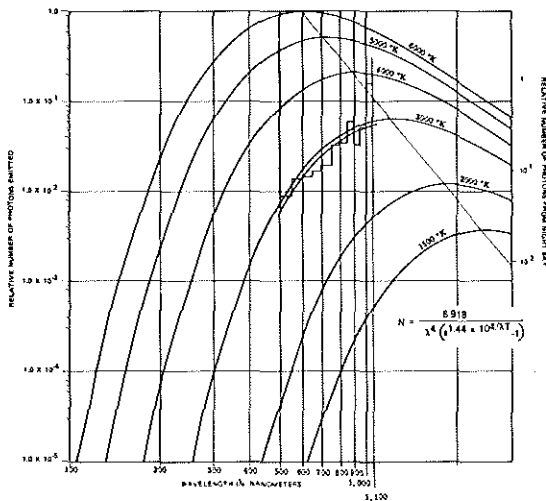


FIGURE 5. COMPARISON OF NIGHT SKY PHOTON COUNT VS. WAVELENGTH WITH BLACKBODY CHARACTERISTICS

Since daytime operation would not require performance at a blackbody color temperature greater than 6000°K, it may be concluded that the viability of a CCD image sensor system depends upon its ability to function within the blackbody color temperature range of 2800°K–6000°K.

BLACKBODY SOURCE DEVICE RESPONSIVITY

The responsivity (ρ) of the type of silicon used in the subject devices has been evaluated as shown in Figure 6. The values of $\rho\lambda$ (spectral responsivity) were taken from measured Fairchild data. It must be noted that the responsivities which may be taken from the graph refer to light which has "gotten into" the silicon. If no special steps were taken to develop a structure receipt to optimize the optical admittance factor, the achievable practical sensitivity could reach only about 35 per cent of the theoretical values shown on the graph.

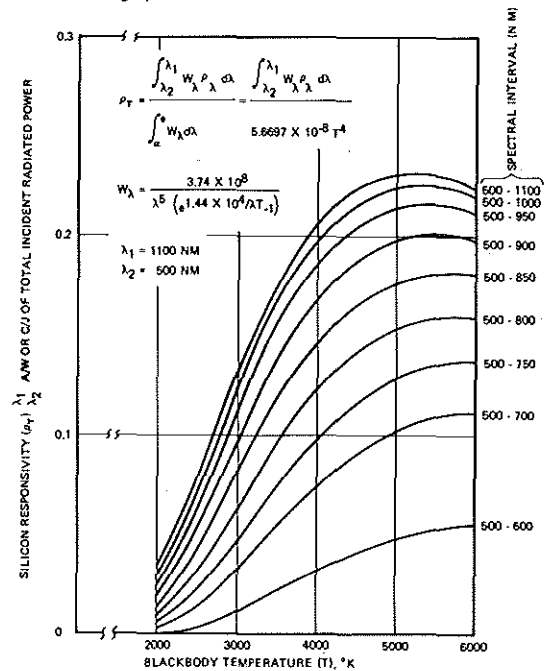


FIGURE 6. SILICON RESPONSIVITY AS A FUNCTION OF BLACKBODY SOURCE TEMPERATURE FOR VARIOUS SPECTRAL INTERVALS

Because of optical interference effects and simple absorption by the several layers of different materials comprising the CCD image sensor structure, the spectral responsivity of a specific device will be dependent upon its construction. (For example, linear devices may require only one layer of polycrystalline silicon, while area devices may require two or more). These effects must be accounted in the determination of specific device responsivity. As an example of what can be accomplished interactively between the system designer and the sensor manufacturer, consider the results of a recent experiment. By using current analytical structure design methods and a newly developed evaluation program, it has proved possible to engineer practical manufacturable layering structures for the subject devices which will more than double the original rather pessimistic responsivity estimate. Twelve such improved structure receipts were selected from a series of 100 evaluated.

Of the twelve, receipt No. 8 was found to be optimum over the blackbody color temperature range of from 2000°K to 6000°K. Data for the optimum improved structure are presented in Figure 7 & 8. The integral evaluated in this latter case includes the expression T_λ so that the resultant responsivity values are those which can be attained when all reflection and unwanted absorption losses are accounted.

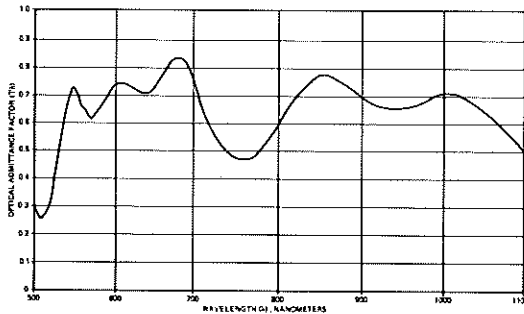


FIGURE 7. OPTICAL ADMITTANCE FACTOR FOR RECEIPT 8

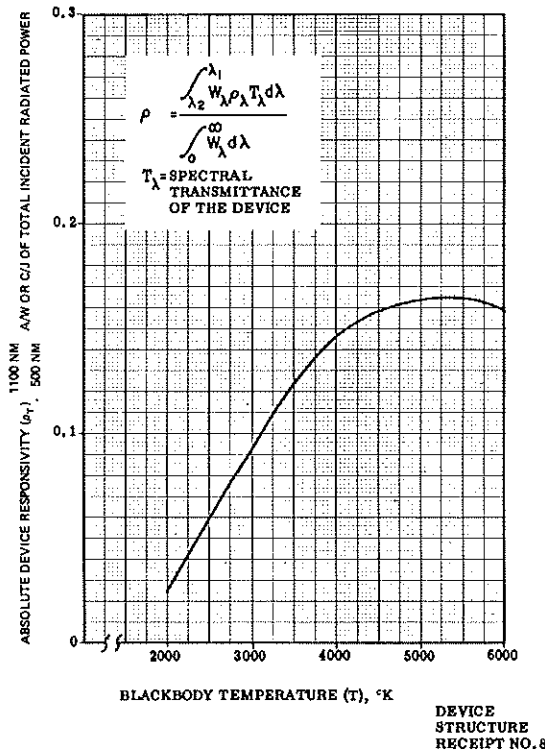


FIGURE 8. DEVICE SENSITIVITY AS A FUNCTION OF BLACKBODY SOURCE TEMPERATURE FOR THE SPECTRAL INTERVAL 500- 1100 NANOMETERS

While Structure Receipt No. 8 was the best of the group developed, the differences in performance among the selected group of twelve were relatively small. Subsequent manufacture of devices in accordance with the model specifications yielded sensors whose responsivity equaled or exceeded the predictions. In most instances the fortuitous relationship between system designer and device manufacturer cited in this example will more than likely not exist. It remains crucially important for the system designer to know, evaluate and understand the impact of the illumination source/ sensor responsivity relationship on system performance.

SIGNAL TO NOISE MODEL

The analysis of sensor performance in a system is directly tied to the definition of a suitable system input signal to noise ratio (S/N). Although the two general classes of CCD image sensors (linear devices and area devices) operate in somewhat different ways, it is possible to develop such a model applicable to both. The model may also be applied to the moving image integrating mode device, which can be considered as a special case of the linear sensor type.

The signal to noise model presented here was originally developed for use in calculating predicted performance for the moving image integrating mode type of device. In the model, the term (η) is used to designate the number of integrations. The same model is directly applied to linear devices (in this case ($\eta = 1$)) and with a somatic difference to area sensors where the readout of several frames may be integrated by the eye-brain combination of the observer via a visual display. In this latter instance (η) is redefined as the number of visual integrations performed within the integration period of the eye (≈ 0.2 Seconds).

A fundamental requirement for an imaging system analysis is the derivation of a mathematical expression for the calculation of the resultant system input signal-to-noise ratio in terms of the various system and mission parameters.

This expression will first be developed for an ideal system, i.e., one that contributes no system noise. For the ideal noiseless system, the only noise present is the statistical noise of the signal itself. A sufficiently close approximation is obtained by considering that part of the system having the lowest discrete unit count as a representation of the signal value. In an electro-optical system, that point is usually the electron stream immediately following the photoelectric conversion whether this be by a photo cathode emitting electrons in a vacuum tube or generation in a solid state photoconductor. The number of electrons representing the "signal" and the number of electrons representing the "noise" or "signal uncertainty" are the valid quantities to use. The signal-to-noise ratio is then:

$$(S/N) = \frac{\epsilon_s}{\epsilon_n}$$

where ϵ_s = the number of electrons representing the "signal" and ϵ_n = the number of electrons representing the "noise".

In an imaging system, where the ultimate final interpretative receiver and decision mechanism is the eye - brain combination, the "signal" which is meaningful is the difference in gray level between one small scene area and an adjacent one - the image characteristics which the brain has been trained to interpret as "detail", as distinguished from the interpretation of "no detail" for an area of uniform gray level. Therefore, for a meaningful analysis of a system's capabilities, it is customary to analyze its treatment of certain specific targets - such as the USAF standard tri-bar target. For such a target, which contains repetitive lines and spaces, we consider one line pair, i.e., one bar and one space and then the signal is:

$$\epsilon_s = \epsilon_{s_{\max}} - \epsilon_{s_{\min}}$$

where $\epsilon_{s_{\max}}$ = the number of electrons from the brighter area, i.e., a bar.

$\epsilon_{s_{\min}}$ = the number of electrons from the dimmer area, i.e., the space between bars.

and the noise is:

$$\epsilon_n = \sqrt{\epsilon_{s_{\max}} + \epsilon_{s_{\min}}}$$

To evaluate these terms:

$$\epsilon_{s_{\max}} = 6.24 \times 10^{18} \rho I_{i_{\max}} P \eta t a_{\text{bar}}$$

$$\epsilon_{s_{\min}} = 6.24 \times 10^{18} \rho I_{i_{\min}} P \eta t a_{\text{space}}$$

where: ρ is the photo-electric responsivity in amp/watt

$I_{i_{\max}}$ is the illuminance of the bar on the image plane

$I_{i_{\min}}$ is the illuminance of the space on the image plane

P is the photometric to radiometric conversion factor for the particular radiation

$\eta \cdot t$ is the integration time (η = number of integrations, t = element exposure time)

a_{bar} is the area of the bar in the image plane

a_{space} is the area of the space in the image plane

For the target referenced, and for this analysis:

$$a_{\text{bar}} = a_{\text{space}} = a$$

σ = the number of "pixels" in a bar

where, by definition:

a = area of a pixel

$a = \delta^2$ (assumed square pixel)

δ = photosite side dimension

For convenience, substitute C for $6.24 \times 10^{18} \rho P \eta t a \sigma$

The expression for the Signal to Noise Ratio is:

$$\frac{(\epsilon_{s_{\max}} - \epsilon_{s_{\min}})}{\sqrt{\epsilon_{s_{\max}} + \epsilon_{s_{\min}}}} = \frac{C (I_{i_{\max}} - I_{i_{\min}})}{\sqrt{C (I_{i_{\max}} + I_{i_{\min}})}}$$

The Sensor MTF describes the ratio of an output signal to the input signal. It is a useful parameter for analyzing the capabilities of imaging systems. The MTF is a spatial frequency dependent term and applies to the sinusoidal signal component for a particular spatial frequency. When dealing with periodic bar targets the MTF is somewhat different than for sinusoidal ones. However, the implicit simplifying assumption that the MTF is not different has been made here. It follows then that the sensor MTF, denoted by M , is as follows:

$$M = \frac{\frac{(I_{\max} - I_{\min})_{\text{out}}}{(I_{\max} + I_{\min})_{\text{out}}}}{\frac{(I_{\max} - I_{\min})_{\text{in}}}{(I_{\max} + I_{\min})_{\text{in}}}}$$

where I_{\max} and I_{\min} are the signal intensities for the maximum and the minimum signals respectively. Since the system is assumed to be linear and since no energy is either added or lost, but is only redistributed between the bars and spaces,

$$(I_{\max} + I_{\min})_{\text{out}} = S (I_{\max} + I_{\min})_{\text{in}}$$

where S is a scale factor:

$$\frac{M \cdot S (I_{\max} - I_{\min})_{\text{in}}}{S (I_{\max} + I_{\min})_{\text{in}}} = \frac{(I_{\max} - I_{\min})_{\text{out}}}{(I_{\max} + I_{\min})_{\text{out}}}$$

or, cancelling out the denominators, which are equal:

$$M \cdot S (I_{\max} - I_{\min})_{\text{in}} = (I_{\max} - I_{\min})_{\text{out}}$$

Substituting in the sensor signal-to-noise expression,

$$\frac{\epsilon_s}{\epsilon_n} = \frac{C \cdot S (I_{\max} - I_{\min})_{\text{in}} \cdot M}{\sqrt{C \cdot S (I_{\max} + I_{\min})_{\text{in}}}}$$

$$(I_{\max})_{\text{in}} = I \cdot R_{\max}$$

$$(I_{\min})_{\text{in}} = I \cdot R_{\min}$$

Where

I = illuminance of the bar in the object plane

R_{\max} = Reflectance of the bar

R_{\min} = Reflectance of the space

$$(I_{\max} - I_{\min})_{\text{in}} = I (R_{\max} - R_{\min})$$

$$(I_{\max} + I_{\min})_{\text{in}} = I (R_{\max} + R_{\min})$$

Substituting:

$$\frac{\epsilon_s}{\epsilon_n} = \frac{C \cdot S \cdot I \cdot M (R_{\max} - R_{\min})}{\sqrt{C \cdot S \cdot I (R_{\max} + R_{\min})}}$$

The scale factor of a linear imaging system is:

$$S = \frac{(I)_{\text{out}}}{(I)_{\text{in}}}$$

where

$(I)_{\text{out}} = I_i$ = the image illuminance

$(I)_{\text{in}} = B_o$ = the object brightness

The relationship is:

$$I_i = \frac{B_o}{4(T\#)^2}$$

$$S = \frac{1}{4(T\#)^2}$$

Where there is an intervening atmosphere,

$$CSI = \frac{6.24 \times 10^{18} \rho^2 \eta \alpha \sigma T}{4(T\#)^2} = Q$$

where T is the atmospheric transmission

or:

$$\left(\frac{S}{N}\right) = \frac{\epsilon_s}{\epsilon_n} = \frac{Q (R_{\max} - R_{\min}) M}{\sqrt{Q} \sqrt{(R_{\max} + R_{\min})}} = \frac{\sqrt{Q} (R_{\max} - R_{\min}) M}{\sqrt{R_{\max} + R_{\min}}}$$

for the noiseless case.

When additional "non-quantum" noise is present, the expression becomes more complex:

$$\left(\frac{S}{N}\right) = \frac{\epsilon_s}{\epsilon_n} = \frac{Q (R_{\max} - R_{\min}) M}{\sqrt{Q} \sqrt{(R_{\max} + R_{\min})} + \sigma \beta^2}$$

Where β is the number of uncancelable noise electrons per pixel referred to the input of the on-chip amplifier.

The relationship between the value of the quantity (S/N) as derived here and system "resolution" ultimately involves an observer. Whether that observer looks at a video "soft copy" presentation or a "hard copy" output will depend upon system-specific requirements.

Threshold observed signal-to-noise ratio values required for an observer to perceive image information for both "soft copy" (live) and "hard copy" displays have been extensively investigated over the past few decades. Refs 4, 5. Although psychophysical aspects of the perception problem have yet to be established on a firm theoretical basis, a number of investigators have successfully demonstrated system analytical techniques based on models of the vision process formulated to conform with the results of numerous controlled experiments. Results specifically applicable to CCD imaging sensor systems include:

Simple aperiodic shapes such as disks and squares viewed against a uniform background have been found to require signal-to-noise ratios perceived by the observer of $\cong 5:1$ for observers viewing images with temporally-fixed noise and signal patterns (i.e., hard copy or stored single-frame television displays). In this case (S/N) is given by the signal to RMS noise ratio determined for the total aperiodic image area and an equivalent area of adjacent background. The "signal" in the photographic image case is the mean difference in events (i.e., darkened specks on film) between the image and background areas, while the noise is determined by the RMS value of background (non-signal) noise events for both areas.

Photographic images of periodic test patterns, such as U.S.A.F. three bar test targets, may be resolved with threshold (S/N) values $\cong 4:1$ where (S/N) is determined over image and background areas equivalent in size to the area of a single test pattern bar.

Ref 6. The criterion adapted here was 50 per cent probability for the detection of line structure in one of the two orientations of three bar images presented to the observer.

In addition to the above, results for television imaging show that long rectangular areas (viewfield angular subtense $0.5^\circ \times 6^\circ$) are detected with threshold observed (S/N) values $\cong 3:1$.

The latter result suggests a remarkable observational ability for effective integration over the entire length of long lines. For a rectangular area of height = 20 x width ($\sigma = 20$) the corresponding elemental (S/N) value for an area of height equal bar width is only $3\sqrt{20} \cong 0.7:1$. These experimental results are confirmed by the critical nature of coherent signature problems, which must be controlled to eliminate streaking in the display output of line-scanning systems.

From the foregoing, we can deduce that "worst case" (S/N) requirements correspond to the detection of objects with image dimensions at the array approaching the minimum sample aperture size of the CCD sensor chip.

Investigation of threshold signal-to-noise ratio requirements for "night vision" applications have been primarily concerned with "live" viewing conditions, with the observer viewing images containing temporal noise variations. Threshold observed (S/N) values appropriate to the latter viewing condition are computed using an assumed value for the effective eye integration time, i.e., 0.1 to 0.2 second for normal display illuminance levels.

The (S/N) model developed above includes the term (η), the number of picture integrations. These integrations may be obtained thru the use of a moving image mode integrating sensor chip, or thru the addition of information in the brain of the observer viewing a "live" display. In the latter case, the number of integrations is limited by the integration time of the eye, while in the former it is a function of sensor chip construction. In either event, the integration effect is accounted in the model, so that a minimum value for (S/N) corresponding to a 50 per cent probability of "resolution" is $\cong 4$.

Similarly, the (S/N) model considers the aspect ratio of a line or periodic target, since the number of pixels in a "bar" (σ) is included in its calculation. This also causes convergence of the required (S/N) to $\cong 4$ for 50 per cent probable "resolution". While no hard and fast rule may be established to relate (S/N) values as calculated from the derived model to "resolution", the selection of (S/N) = 4 as a minimum requirement for periodic targets has been applied with considerable success.

OPERATIONAL PARAMETER SPACE

Having derived the appropriate system input signal-to-noise ratio (S/N), it is necessary to determine the interrelationships among those sensor characteristics that effect the quantities in the expression:

$$(S/N) = \frac{Q (R_{\max} - R_{\min}) M}{\sqrt{Q} \sqrt{(R_{\max} + R_{\min})} + \sigma \beta^2}$$

Let us examine each of the quantities in that expression and the effects of sensor characteristics upon their quantification.

FACTORS IMPACTING SIGNAL LEVEL

The quantity "Q" has been defined as:

$$Q = \frac{6.24 \times 10^{18} \rho P \cdot I \eta \alpha \sigma T}{4(T\#)^2}$$

6.24×10^{18} is the number of electrons per coulomb and is constant.

" ρ " is the responsivity of the sensor in coulombs/joule or amps/watt. This quantity varies with the wavelength or color temperature of the illumination, which must be considered in selecting the proper value for ρ . Rho is based on a 100 per cent area utilization factor in the chip.

" $P \cdot I$ " is the product of the scene illumination in foot candles and a Photometric-Radiometric conversion constant which in turn is dependent upon illumination color temperature. It assumes that the illumination source is a blackbody. If this is not the case, the values for ρ and the equivalent of $P \cdot I$ (in watts cm^{-2} on the scene) must be appropriately computed. The type and color temperature of the illumination also effects such parameters as crosstalk, and array MTF (m_{array}).

" η " is the number of image integrations - either during image gathering (as with a moving image integrating mode chip) or during display (based on the time-constant of the eye). System requirements for specific light level performance or display characteristics may influence the needed value.

" t " is the elemental exposure time in seconds. This will be determined by the frame repetition rate or the linear device read-out rate in frames or lines per second respectively. In terms of system operation, these rates may be established from such diverse requirements as vehicle rate, scene overlap, ambient light level, or display frequency.

" α " is the area of a pixel. It applies to the entire area of a picture element (active area plus inactive area). Note that responsivity (ρ) is also computed on the basis of total pixel area. Coupled with the object space system resolution requirements, the pixel size tends to define the required optical scale of the system.

" σ " is the number of pixels in the area of a bar of a (square wave or tribar) bar type of target.

" T " is the atmospheric transmission.

" $(T\#)$ " is the (F#) of the optical system divided by the square root of the optical transmission of that system.

The quantities most amenable to trade-off in the course of system analysis are exposure time (t), $(T\#)$, and σ . The latter is directly connected with image resolution.

The maximum and minimum scene reflectances R_{max} and R_{min} are most likely either specified or implied by the system specification. In any event, they are not variable from the system trade-off analysis standpoint. However, their absolute values, as well as the target contrast ratios, are important in system analysis.

MODULATION CONSIDERATIONS

The quantity M which appears in all S/N computations is used to designate the Modulation Transfer Function of the "system" and consists of the following factors:

$$M = (m_{\text{optics}}) (m_{\text{motion}}) (m_{\text{array}})$$

It should be noted immediately that the evaluation of "M" does not contain constant terms for either the modulation of the optics or the scene contrast ratio. Even though, for simplification of calculations a constant m_{optics} may be assumed, the quantity is spatial frequency dependent and must ultimately be recognized as such. The scene contrast ratio (in terms of R_{max} and R_{min}) is also accounted for in the (S/N) computation, but not as a "modulation" term.

The first of the cascaded values which go to make up the system MTF (M) to be considered is m_{optics} . System designers are familiar with the variation of m_{optics} with spatial frequency. However, a note of caution if appropriate. Many attempts are made to configure CCD image sensor based systems around photographic optics which were designed for optimum performance within a different spectral domain than the "wide-open" silicon response spectrum. The values for m_{optics} used in system performance prediction must correspond to the weighted spectral interval appropriate to the operational system.

The evaluation of the effects of image motion must be conducted differently for cases where such image motion is inadvertent (due to platform instability, object motion etc) and where the motion of the image past a linear sensor is implicit in the generation of one dimension of the picture (strip mode or panoramic cameras for example).

In the first instance, where undesired image motion during exposure is encountered, the MTF due to motion (m_{motion}) may be evaluated from the expression:

$$m_{\text{motion}} = \frac{\text{Sin}(\pi \theta \eta f R t)}{(\pi \theta \eta f R t)}$$

where θ is the image motion rate in radians per second, f the lens focal length in units of length consistent with R , the spatial frequency of interest in line pairs per unit length.

Where image motion past a linear sensor is used to generate one dimension of the "picture", the linear rate of image motion (V) and the exposure time (t) combine to establish the value for m_{motion} for a given spatial frequency (R)

$$m_{\text{motion}} = \frac{\text{Sin}(\pi V R t)}{\pi V R t}$$

Note that the number of integrations no longer forms a part of the expression.

For a given spatial frequency R , it can be shown that

$$(S/N)_R \approx \frac{\text{Sin}(\pi W)}{\pi W}$$

where W is the image motion in lp/sec. and also that:

$$(S/N)_R = \text{max when the argument Sin}(\pi W) = 1 \text{ or, } Wt = 1/2R$$

which implies that the maximum $(S/N)_R$ is obtained when one line readout is made per $1/2R$ wide line progression in the image.

Strictly speaking, the optimization applies only to the spatial frequency R . A small gain in "resolution" may be obtained by reading out the array more than once per line progression in the image even though this degrades the value of (S/N) at spatial frequency R . This follows from the fact that even for a value of R corresponding to the Nyquist limit (the limiting geometrical unambiguous resolution of the sensor is set at the Nyquist limit) the sensor may well exhibit response beyond that frequency. With more than one readout per line progression, a greater amount of these higher frequency components may be passed by the system resulting in sharper edges even though the (S/N) at spatial frequency R is no longer optimum. In instances where there is an image motion error associated with the picture generation by a scanning linear sensor, the MTF contribution of the error can be calculated from the same general sinc function as that given previously for inadvertent image motion viz:

$$m_{\text{motion}} = \frac{\text{Sin}(\pi\theta\eta fR)}{\pi\theta\eta fR}$$

In this instance θ is the image motion error rate in radians per second, and η is normally unity for a linear sensor.

The MTF of the array (m_{array}) is a quantity which varies not only as a function of sensor geometry, but with several operational characteristics as well. Also the combinations of operating characteristics possible within the permissible working range of a given sensor may result in very significantly different values for m_{array} . The MTF of the array must be modeled in accordance with the conditions of use in the system and the appropriate values used in the system performance prediction calculations. Different types of devices (frame-transfer devices and interline transfer devices for example) exhibit different array MTF characteristics. Ref 7. The specific properties of each system candidate array should be investigated using whatever device MTF model is appropriate. As an example, an MTF model for a typical linear array under one set of operating conditions is presented in Figure 9. The curve labeled "model" represents the "most likely" phase relationship between a square wave target and the array. Experimental data points obtained from 1×500 element linear arrays are also shown in the Figure. It may be seen that the experimental points agree reasonably well with the derived model for the conditions assumed for this system.

Unfortunately, there is no single characteristic curve of m_{array} for a given image sensor device. Instead, the parameter varies as a function of several system-connected operational characteristics. The most significant of these areas effecting this spatial frequency dependent parameter includes:

- Array Geometry
- Readout Rate
- Illumination Color Temperature (Cross Talk)
- Charge Transfer Efficiency (which in turn is effected by)
 - Signal Level
 - Operating Temperature
 - Device Type

Succinct questions as to these sensor and system characteristics must be asked and answered by the system designer in the course of preparing the array MTF model to be used in subsequent system analysis. Failure to generate a model of the necessary accuracy can lead to grossly inaccurate performance predictions.

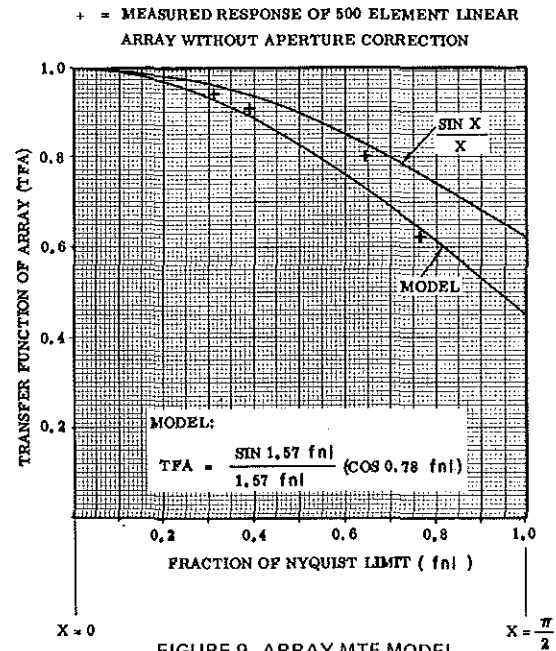


FIGURE 9. ARRAY MTF MODEL

NOISE CONSIDERATIONS

The final quantity in the expression for (S/N) is (β) , the number of uncancelable noise electrons referred to the input of the on-chip amplifier associated with each pixel readout. This constitutes the non-quantum noise of the sensor and is Root Sum Squared with the quantum noise in the determination of (S/N) .

No attempt is made in this paper to establish all the physical sources of noise within a CCD imaging sensor chip, since from a system designer's point of view the precise source of the noise is of only academic interest. There are however two generalized sources of noise electrons: Those associated with thermal generation within the sensor chip, and those having their origin elsewhere.

Thermally generated noise electrons are the result of dark current statistics (uniform dark current itself can be electrically canceled) and dark current non-uniformities. While quite low values of dark current density ($10\text{nA}/\text{cm}^2$ is not atypical) are commonly measured, the mistake of multiplying this density times the pixel area to determine the dark signal must be assiduously avoided. It must be remembered that the photosensitive area is not the only portion of the sensor real-estate contributing to the dark signal. So while on the basis of $10\text{nA}/\text{cm}^2$ dark current density one might compute the dark signal for a pixel to be of the order of from 10 to 100 electrons in a $53\ \mu\text{s}$ integration time the actual dark signal for a commercial device with these characteristics averages more nearly 2500 electrons dark signal with a dark signal statistics noise contribution of 50 electrons (at 25°C).

Dark signal non-uniformity is generally described in terms of "per cent". This does not refer to per cent of average dark signal, but to per cent of saturation signal. Variations in dark signal of as much as 1 per cent of saturation are not uncommon in today's devices operating at 25°C . For a sensor with a pixel which is saturated by 250,000 electrons, this corresponds to 2500 electrons. Such a number, though

large, is not particularly bothersome when the device is operating at signal levels of 50 per cent saturation or above. However, let the signal level drop to 1 per cent of saturation, and the impact of the dark signal non-uniformity is severely felt.

The system designer has within his control an option whereby the effects of thermally generated noise may be greatly minimized or essentially eliminated. He may elect to cool the sensor. By "Rule of Thumb", the number of thermally generated electrons is halved for every 9°C drop in operating temperature. A plot of the Dark Charge Temperature Characteristic for a sample device is presented in Figure 10. Since cooling is effective against variations in dark signal as well as against dark signal itself, the 2,500 noise spike electrons per pixel given in the previous example (with the sensor operating at 25°C) would be reduced to 20 noise electrons by cooling the sensor to -38°C. Meanwhile, the average dark signal level of the example would have similarly been reduced from 2500 to 20 with the dark signal statistics noise equal to 4.5 electrons per pixel.

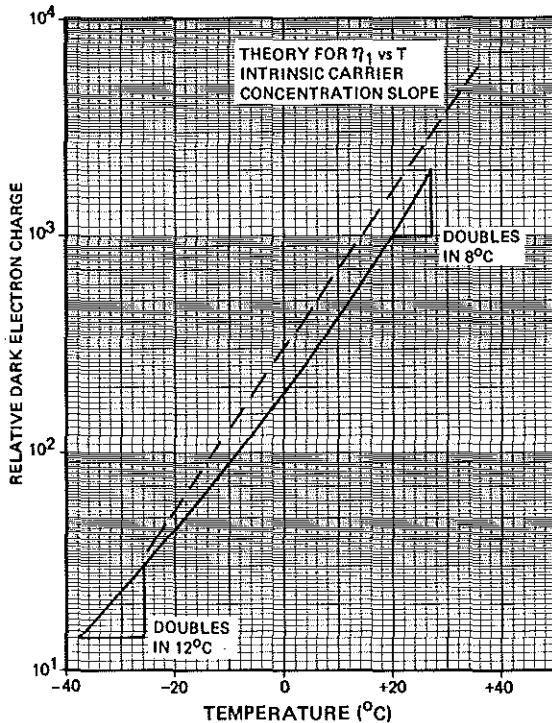


FIGURE 10. TYPICAL DARK CHARGE TEMPERATURE CHARACTERISTICS

Whether or not cooling the sensor will offer a system advantage depends upon what forms the predominant noise source in the specific sensor device being considered. In many instances, the dominant noise source is in the on-chip amplifier and/or the way in which the sensor array is read out. When such is the case, the effects of cooling are to eliminate the few large dark signal variation spikes and to lower the overall RMS noise level slightly, but to not dramatically improve the imagery obtained. Cooling of the

sensor chip does have a minimizing effect on other (non dark-signal associated) noise sources. Both kT/c noise and Johnson noise for example are reduced somewhat when the sensor is cooled. However, the effect on such noise sources is small compared to the effect on dark signal related noises. Therefore, the system decision as to whether or not to cool a given sensor chip will most probably be regulated by the relative importance of dark signal associated noise.

Of the types of on-chip amplifiers in use today or contemplated for the near future, two generalized categories exist: The gated charge integrator (used either alone or in combination with an on-chip compensation amplifier), and the floating gate amplifier (the latter can be of one or multiple stages, with the multiple stage version being described as a distributed floating gate amplifier). The number of noise electrons per pixel readout associated with specific amplifiers may vary from as many as 2000 to as few as 20. Generally speaking the relative ranking (from least to most "noisy") is; distributed floating gate, floating gate, gated charge integrator with on-chip compensation amplifier, and the uncompensated gated charge integrator.

One might reasonably ask why a single amplifier type (logically the least "noisy") is simply not settled down upon for all applications, and the entire matter set to rest for all time. Unfortunately, low noise demands a price, and that price is usually a reduced amplifier saturation threshold. The implication of this for system applications is reduced in-scene dynamic range reproduction.

From a system designer's point of view it would be optimum to have each sensor chip come equipped with multiple on-chip amplifier options so that the optimum amplifier could be switched on-line with varying operational conditions. Experimental sensor chips incorporating such a feature have been produced.

The noise metric used in the (S/N) model involve the quantity (β) which represents the number of uncancelable noise electrons referred to the input of the on-chip amplifier. Deriving this quantity from published device data at times presents a challenge. The approach usually taken is to reduce the published noise equivalent signal or noise equivalent exposure data to an equivalent number of electrons. If cooling below the temperature at which values for these quantities were obtained is anticipated, the specific effects of this cooling on (β) must be calculated or obtained from the manufacturer.

DETECTIVE QUANTUM EFFICIENCY CONSIDERATIONS

A part of any system analysis which considers the use of CCD imagery sensors logically involves comparison with other sensor types. One such type of comparison involves the use of the quantity Detective Quantum Efficiency (DQE). While DQE does not constitute a single simple figure of merit, it is one significant performance characteristic. It describes how efficiently the detector makes use of the information present in a photon image. (Ref 8). It may be mathematically defined as:

$$DQE = \frac{(S/N)_{out}^2}{(S/N)_{in}^2}$$

In this instance the value of (S/N) calculated for our model represents (S/N) out, while the ideal (S/N) inherent in the signal sensed by a perfect sensor represents the (S/N) in.

$$\text{Now, } (S/N)_{out} = \frac{Q (R_{max} - R_{min}) M}{\sqrt{Q (R_{max} + R_{min}) + \sigma\beta^2}}$$

where

$$Q = \frac{6.24 \times 10^{18} \rho_T P \cdot I \eta \alpha \sigma T}{4(T\#)^2}$$

For the ideal case,

$$(S/N)_{in} = \frac{Q^* (R_{max} - R_{min}) M}{\sqrt{Q^* (R_{max} + R_{min})}}$$

where

$$Q^* = \frac{6.24 \times 10^{18} \rho_T^* P \cdot I \eta \alpha \sigma T}{4(T\#)^2}$$

and

ρ_T^* = Blackbody responsivity of a 100% quantum efficient detector at a blackbody temperature T

$$\rho_T^* = \frac{\int_{\lambda_2}^{\lambda_1} 8.068 \times 10^{-1} W_\lambda d\lambda}{5.6697 \times 10^{-8} T^4}$$

and,

$$W_\lambda = \frac{3.74 \times 10^8}{\lambda^5 (e^{1.4388 \times 10^4 / \lambda T} - 1)}$$

also,

$$Q^* = Q \frac{\rho_T^*}{\rho_T}$$

Now, by definition (S/N) for a "noiseless" system is \sqrt{Q} when all modulation, reflectivity, and transmission terms are disregarded. For this case then, $(S/N)_{in}^2 = Q^*$

and

$$(S/N)_{out}^2 = \frac{Q^2}{Q + \beta^2}$$

and

$$DQE = \frac{Q^2}{Q^* (Q + \beta^2)}$$

For completely "real world" cases,

$$(S/N)_{out}^2 = \frac{Q^2 (R_{max} - R_{min})^2 M^2}{Q (R_{max} + R_{min}) + \sigma \beta^2}$$

and

$$(S/N)_{in}^2 = \frac{Q^*^2 (R_{max} - R_{min})^2 M^2}{Q^* (R_{max} + R_{min})}$$

from which

$$DQE = \frac{Q^2}{Q^*} \times \frac{(R_{max} + R_{min})}{[Q(R_{max} + R_{min}) + \sigma \beta^2]}$$

As an example we have taken the case of an ideal detector and plotted its responsivity alongside that of a CCD imaging sensor having the characteristics represented of Receipt 8. These data are shown in Figure 11.

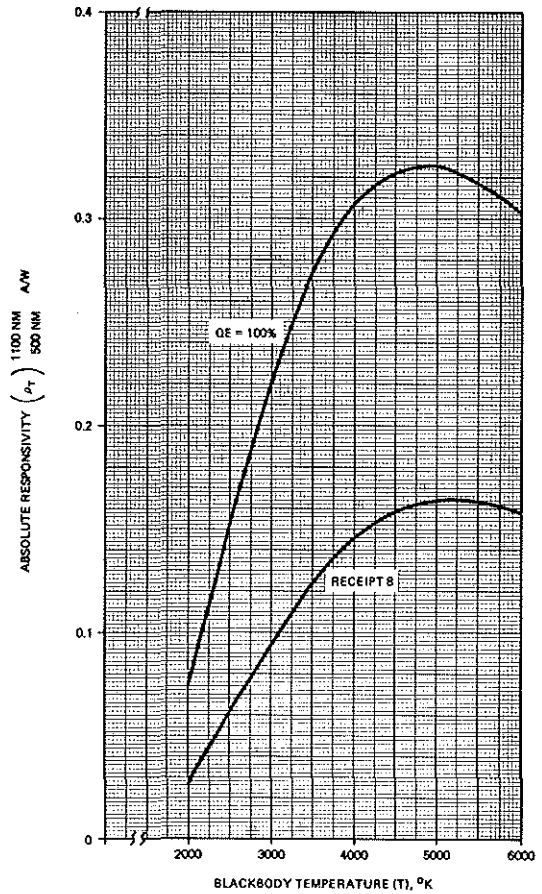


FIGURE 11. RESPONSIVITY AS A FUNCTION OF BLACKBODY TEMPERATURE FOR REAL AND IDEAL DEVICES

For a situation where:

- T = 6000°K
- R_{max} = 0.5
- R_{min} = 0.25
- β = 40 electrons
- ρ = *Receipt 8
- σ = 5

The Detective Quantum Efficiency is computed to be a function of Q as shown in Table I.

TABLE I

RELATIONSHIPS BETWEEN SIGNAL LEVEL AND DQE FOR ONE EXAMPLE

Q ELECTRONS PER SIGNAL AREA	ELECTRONS PER PIXEL	Q* IDEAL ELECTRONS PER SIGNAL AREA	DQE
100,000	20,000	190,000	0.475
10,000	2,000	19,000	0.254
1,000	200	1,900	0.045
100	20	190	0.005

EXAMPLE

The following example of system calculations is presented not as a solution to any particular "real world" problem, but rather as a guide to the application of the methods described in the previous sections of this paper. The device characteristics chosen are not specifically representative of a particular sensor, but fall within the current State of the Art.

SYSTEM REQUIREMENTS

A low altitude reconnaissance aircraft is to fly at an altitude of 3000 feet at a maximum V/H of 0.15 knots per foot.

Scene illumination will be daylight, down to sun angles corresponding to 100 foot candles scene illuminance (minimum) with cloud cover.

Scene contrast ratios of 2:1 and above are anticipated, with average scene reflectivities of 0.3.

Ground resolution of 6" per line pair is desired.

Continuous angular coverage of ±20° from nadir is required.

TENTATIVE SYSTEM CONCEPT

As a starting point the system designer might consider a strip mode type of system consisting of a series of linear sensor chips arranged to form a (optically or electronically) contiguous line in the image plane of a vertically oriented objective lens. It is necessary to check this concept against available sensor characteristics.

ASSUMED SENSOR DEVICE SPECIFICATIONS

- Type: 1 x 1500 pixel linear chip
- Pixel Size: 0.0007" x 0.0007"
- Active Pixel Area: 100%
- Responsivity: In accordance with Figure 8
- Dynamic Range: 1000:1
- Saturation: 300,000 electrons
- Average Dark Signal: 50 electrons/μSec/Pixel at 25°C
- Dark Signal Non-Uniformity: 1% of Saturation
- Readout Rate: 0.1 – 6.0 M Samples/Sec
- Array MTF: In accordance with "Model" Figure 9 within 0.1 – 6.0 M Sample/Sec readout rate
- RMS Noise (excluding dark signal associated noise): 150 electrons/pixel readout when operated between 0.1 – 6.0 M Samples/Sec.

PRELIMINARY SYSTEM ANALYSIS

The requirement for 6"/l.p. ground resolution demands a lens focal length of at least

$$f = \frac{0.0007}{3.00} \times 3000 \times 12 = 8.4 \text{ inches}$$

In order to set the required 6"/l.p. resolution module at 0.84 of the Nyquist limit, a 10" e.f.l. lens is selected.

The ±20° field of view represents a line 7.28 inches long in the focal plane. This requires 7 sensor chips (each with a 1.05" long sensor area). A seven-channel system is therefore tentatively hypothesized.

At the V/H of 0.15 knots/foot and the altitude of 3000 feet, the vehicle velocity V is seen to be 9120 inches per second from which the image velocity using the 10" e.f.l. objective lens calculates to be 2.53 inches per second. V = 2.53.

If each channel is read out once per line progression in the image, the readout rate is

$$RR = 1500 \frac{2.53}{0.0007} = 5.42 \times 10^6 \text{ Samples/Sec and}$$

$$t = 2.76 \times 10^{-4} \text{ Sec.}$$

This falls within the optimum operational range of our hypothetical sensor chip.

At a "sunlight" illumination of 100 foot candles, the scene irradiance may be seen to be (from figure 2) 1.15 x 10⁻³ watts/cm² at T = 6000°K. I·P = 1.15 x 10⁻³.

The responsivity of our sensor (from figure 8) is 0.158 amps/watt at that color temperature. ρ = 0.158.

A preliminary calculation of a value for "Q" assuming a (T#) = √20 lens yields:

$$Q = \frac{(6.24 \times 10^{18})(0.158)(1.15 \times 10^{-3})(2.76 \times 10^{-4})(3.16 \times 10^{-6})(7)}{80}$$

where $\sigma = \frac{5}{(.84)^2} = 7$ because the aspect ratio of the USAF tri-bar target is 5:1, and the required limiting resolution is at 0.84 of the Nyquist limit.

$$Q = 8.65 \times 10^4 \text{ electrons}$$

Calculation of the dark signal yields:

$$\text{Dark Signal} = 50 \frac{2.76 \times 10^{-4}}{10^{-6}} = 1.38 \times 10^4$$

from which the noise in the dark signal is 117 electrons RMS.

If the occasional dark signal noise spike from areas of dark signal non-uniformity is ignored, the RMS noise may be computed to be (exclusive of quantum noise in signal)

$$\beta = \sqrt{117^2 + 150^2} = 190 \text{ electrons}$$

The system resolution corresponding to 6"/lp on the ground is 600 lp/inch or 23.6 lp/mm at the 10 inch (254 mm) focal length selected. At that spatial frequency a specially designed F/4 (T = $\sqrt{20}$) lens should be capable of exhibiting a minimum MTF of 60 per cent throughout the field of view. $m_{\text{optics}} = 0.60$

The MTF of the sensor is taken from Figure 9 for the 0.84 FNL point to be $m_{\text{array}} = 0.58$.

Since the sensor chip will be read out each 2.76×10^{-4} sec, m_{motion} may be computed from:

$$m_{\text{motion}} = \frac{\sin(\pi V R t)}{(\pi V R t)}$$

$$m_{\text{motion}} = \frac{\sin[\pi (2.53) (600) (2.76 \times 10^{-4})]}{\pi (2.53) (600) (2.76 \times 10^{-4})}$$

$$m_{\text{motion}} = 0.74$$

$$M = (0.60) (0.58) (0.74) = 0.26$$

Since the average scene reflectivity is 0.3 and the Contrast Ratio is 2:1 (minimum),

$$\frac{R_{\text{max}} + R_{\text{min}}}{2} = 0.3, \quad \frac{R_{\text{max}}}{R_{\text{min}}} = 2$$

$$\frac{2R_{\text{min}} + R_{\text{min}}}{2} = 0.3 \quad \frac{3R_{\text{min}}}{2} = 0.3$$

$$R_{\text{min}} = 0.2, \quad R_{\text{max}} = 0.4$$

$$(S/N) = \frac{(8.65 \times 10^4) (0.2) (0.26)}{\sqrt{(8.65 \times 10^4) (0.6) + 7 (190)^2}}$$

$$(S/N) = 8.1$$

Since a 4:1 (S/N) ratio is the minimal acceptable for "resolution", the system as outlined passes the first hurdle of parametric viability.

In the interests of brevity, the analysis has been kept to a rudimentary parametric form. The exercise, however, does serve to illustrate how the techniques outlined here may be applied.

BIBLIOGRAPHY

- Ref. 1: Thomas, W., (Editor), 1973, "SPSE Handbook of Photographic Science and Engineering," pp. 13-29., Wiley Interscience
- Ref. 2: RCA Electro-Optics Handbook, 1968, Section 6.
- Ref. 3: Kingslake, R., 1965, "Applied Optics and Optical Engineering," Vol. I, pp. 141-145, Academic Press.
- Ref. 4: Biberman, L.M., (Editor) 1973, "Perception of Displayed Information", Plenum Press.
- Ref. 5: Rose, A., 1948, "The Sensitivity Performance of the Human Eye on an Absolute Scale," J.O.S.A., 38,2.
- Ref. 6: Schade, O., Sr., 1964, "An Evaluation of Photographic Image Quality and Resolving Power," J.S.M.P.T.E., pp. 81-119, 73, 2 February.
- Ref. 7: Barbe, D.F., and Campana, S.B., 1973, "Operational Characteristics of Charge-Coupled Imagers," pp. 216-223., Proceeding of Electro-Optical Design Conf., New York, Sept. 1973.
- Ref. 8: Zweig, H.J., Higgins, G.C., and MacAdam, D.L., 1958, "On the Information - Detecting Capacity of Photographic Emulsions," pp. 926-933 J.O.S.A., 48, 12.